Scripta Materialia 183 (2020) 111–116

Contents lists available at ScienceDirect

Scripta Materialia

journal homepage: www.elsevier.com/locate/scriptamat

Anomalous effect of lattice misfit on the coarsening behavior of multicomponent $L1_2$ phase

Feng He[a,b], Kaiwei Zhang[a], Guma Yeli[b], Yang Tong[c], Daixiu Wei[d], Junjie Li[a], Zhijun Wang[a,*], Jincheng Wang[a,*], Ji-jung Kai[b,e,*]

[a] State Key Laboratory of Solidification Processing, Northwestern Polytechnical University, Xi'an 710072, PR China
[b] Centre for Advanced Nuclear Safety and Sustainable Development, City University of Hong Kong, Hong Kong, PR China
[c] Division of Materials Science and Technology, Oak Ridge National Laboratory, Oak Ridge, TN 37831, United States
[d] Institute for Materials Research, Tohoku University, 2-1-1 Katahira, Sendai, Miyagi 980-8577, Japan
[e] Department of Mechanical Engineering, City University of Hong Kong, Hong Kong, PR China

ARTICLE INFO

Article history:
Received 7 February 2020
Revised 15 March 2020
Accepted 15 March 2020
Available online 30 March 2020

Keywords:
High entropy alloys
Thermal stability
Lattice misfit
Coarsening kinetics

ABSTRACT

The multicomponent $L1_2$ phase in high entropy alloys (HEAs) has shown excellent thermal stability. However, the understanding of its intrinsic origins is limited to the Lifshitz-Slyozov-Wagner (LSW) theory. In the present study, we investigate the influence of lattice misfit, which is not considered in LSW theory, on the coarsening kinetics of the multicomponent $L1_2$ phase. Different from that in most traditional alloys, the coarsening constant of multicomponent $L1_2$ particles decreases with the increasing lattice misfit in HEAs. This finding provides a new view for understanding the sluggish coarsening kinetics of $L1_2$ phase in HEAs.

The stability of precipitates significantly influences the reliability of precipitation hardened alloys under high temperatures [1–4]. Enhancing the microstructural stability, including coarsening resistance, of coherent precipitates has always been attracting scientific attention [5–8]. Zhao et al. [9] showed that the multicomponent $L1_2$ phase in high entropy alloys (HEAs) exhibit better thermal stability than traditional $Ni_3(Al,Ti)$ and $Co_3(Al,W)$ $L1_2$ phases. The coarsening constant of the multicomponent $L1_2$ phase in the $(NiCoCrFe)_{94}Ti_2Al_4$ is 1.82×10^{-28} m^3/s at 800 °C, and is much lower than that of the $L1_2$ phase in the Inconel 939 (2.67×10^{-28} m^3/s at 750 °C). The excellent thermal stability of the multicomponent $L1_2$ phase was then successively verified by other groups in different HEA systems [10–12]. These pioneer works demonstrated that HEAs with coherent $L1_2$ phase are promising candidates for high temperature applications. More recently, Lu et al. [13] reported that the nano-precipitate can effectively stabilize nano-twins in an interstitial HEA, indicating another advantage of nano-sized $L1_2$ phase in enhancing the thermal stability of HEAs. There is an increasing interest, therefore, in understanding the intrinsic origins of the sluggish coarsening kinetics of the multicomponent $L1_2$ phase.

Previous works have made considerable efforts to uncover the coarsening mechanism of multicomponent $L1_2$ phase in HEAs based on the framework of Lifshitz-Slyozov-Wagner (LSW) theory and an agreement has been reached that the coarsening of $L1_2$ phase in HEAs is controlled by volume-diffusion [9–12]. The slow coarsening kinetics of multicomponent $L1_2$ phase is mainly attributed to the sluggish diffusions of component elements and supposed small interfacial energy [9–11]. However, the lattice misfit between precipitate and matrix, which has not been adequately treated in LSW related theories, also plays an important role in the coarsening behavior [14–20]. For example, the increase of lattice misfit significantly decreased the coarsening constant of the $L1_2$ phases in the Ni-Al binary alloys [18] and the Ni-Al-Mo system [20]. Opposite trend was also observed in the Al-Sc system [19]. Although the effect of lattice misfit on the coarsening kinetics is still debatable, it is clear that lattice misfit greatly affects the coarsening rate constant. Furthermore, the lattice misfit also significantly influences the creep properties of alloys by affecting their directional coarsening behavior [18,20]. Therefore, the effect of lattice misfit on the coarsening behavior of multicomponent $L1_2$ phase should be carefully considered to better understand the coarsening mechanisms of $L1_2$ phase in HEAs.

* Corresponding authors.
E-mail addresses: zhjwang@nwpu.edu.cn (Z. Wang), jchwang@nwpu.edu.cn (J. Wang), jijkai@cityu.edu.hk (J.-j. Kai).

https://doi.org/10.1016/j.scriptamat.2020.03.030
1359-6462/

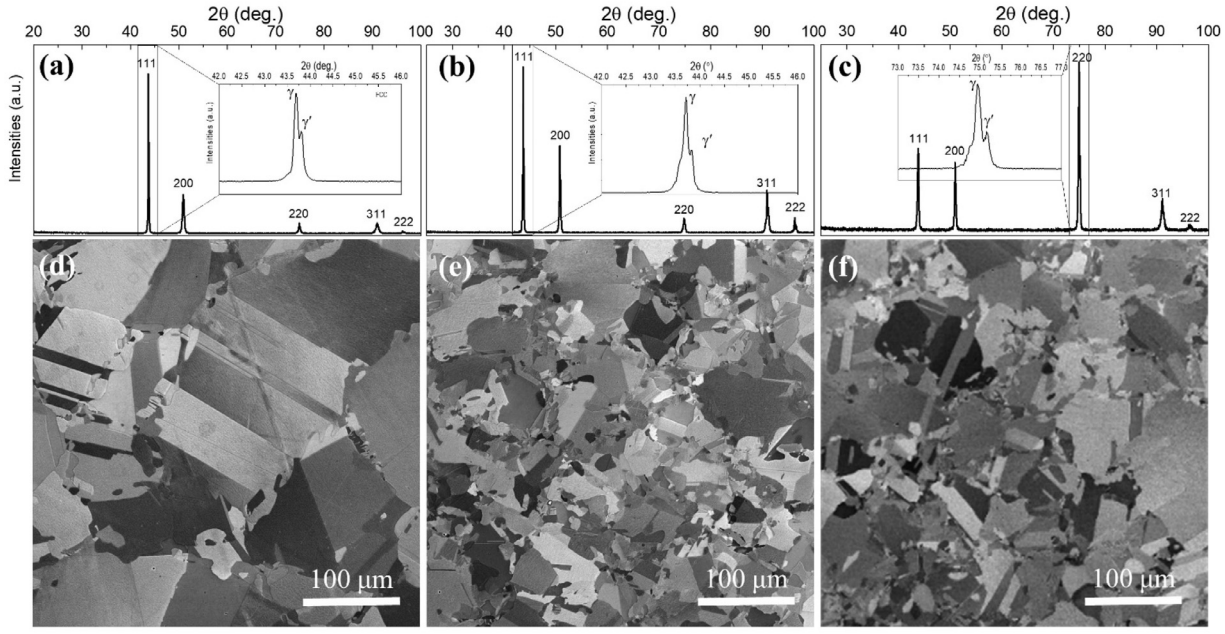

Fig. 1. XRD patterns and SEM-BSE micrographs of the $Ni_2CoCrFeTi_xAl_y$ HEAs aged at 800 °C for 720 h; (a, d) $Ni_2CoCrFeTi_{0.1}Al_{0.2}$ HEA, (b, e) $Ni_2CoCrFeTi_{0.15}Al_{0.15}$ HEA, (c, f) $Ni_2CoCrFeTi_{0.2}Al_{0.1}$ HEA. Other precipitates except $L1_2$ phase cannot be detected neither at grain boundaries nor inside grains after such a long-time exposure at 800 °C.

To this end, this study investigates the effect of lattice misfit between precipitate and matrix on the coarsening behavior in HEAs. In order to experimentally exclude the effect of diffusion and interfacial energy on the coarsening as much as possible, HEAs with very similar compositions are designed. A theoretical model is applied to correct the effect of precipitates volume fraction when comparing the coarsening rate constants and particle size distributions

The novel $Ni_2CoCrFeTi_xAl_y$ ($x + y = 0.3$, $x / y = 0.5$, 1, and 2) HEAs were developed to obtain $L1_2$/matrix microstructure with different lattice misfit values and to compare with reported HEAs as well [9,10]. Elements of Co, Cr, Fe, Ni, Ti, and Al with purity of 99.95% were used as raw materials. Samples were prepared using arc melting and casted into a copper mold with the dimension of 50 × 10 × 5 mm^3.The alloys were melted for five times in an argon atmosphere and then solidified in the water-cooled copper mold. The ingots were solutionized for 2 h at 1200 °C followed by water quenching to obtain single-phase HEAs. The solid solution treated HEAs were cold rolled to ~1.5 mm (~70% thickness reduction) and recrystallized at 1200 °C for 4 min and finally quenched in water. The coarsening behavior of the $L1_2$ phases were investigated by aging the recrystallized HEAs at 800 °C for 24 to 720 h. Water-quenching was immediately performed when the aging process finished to keep the high-temperature microstructure. The SEM samples were prepared by grinding, polishing in diamond suspension, and final polishing in colloidal silica suspension and then analyzed by scanning electron microscope equipped with BSE detector (SEM, Tascan MIRA3). These samples were then used to conduct X-Ray diffraction (XRD) measurement using Rigakud/max-2550. The XRD patterns are obtained from 25 to 100° with scan rate of 4°/min. In order to ensure the precision of the lattice constant, high-resolution XRD test was carried out from 88.5 to 93.5° with a scan step of 0.001° and scan rate of 0.09°/min and a monochrometer is used to eliminate the $K\alpha 2$and $K\beta$ contributions [21,22]. The details of the accuracy of this method was discussed elsewhere [23]. ImageJ software is used for image analysis.

Fig. 1 shows the XRD patterns and microstructure of the HEAs aged at 800 °C for 720 h. XRD patterns of the three HEAs in Fig. 1 indicated a dual-phase microstructure with main diffraction peaks representing disordered FCC phase and side peaks representing ordered $L1_2$ phase (as shown in the enlarged insets). High-resolution XRD test were carried out at the position of (311) peak to obtain the lattice parameters of the matrix and $L1_2$ phase (Fig. S1 and Table 1). One can see that with the increased Ti/Al ratio, the absolute value of lattice misfit increased from 0.19% to 0.24%. It should be noted that the lattice misfits of HEAs in Table 1 were all obtained at room temperature. Although the temperature will influence the value of lattice misfit, it has been proved that the difference in lattice misfit between room temperature and 800 °C is negligibly small [24]. The BSE images in Fig. 1 present the coarsened microstructures of the three $Ni_2CoCrFeTi_xAl_y$ HEAs. The non-uniformity of grain sizes among the three HEAs should be due to the effect of precipitates on the grain boundary migration [12]. No other phases were observed at grain boundaries or inside the grains, indicating a single matrix/$L1_2$ microstructure was obtained.

Fig. 2 shows the evolution of $L1_2$ phase as a function of aging time in the three $Ni_2CoCrFeTi_xAl_y$ HEAs. The $L1_2$ phase in $Ni_2CoCrFeTi_{0.1}Al_{0.2}$ HEA possessed spherical shape, small average size (~ 10 nm), and high number density after aging for 24 h (Fig. 2a_1). The particle size increased while the number density decreased with the aging time, as shown in Fig. 2a_1–a_4. The shape of the $L1_2$ phase remained spherical till 720 h at 800 °C. Similar results had been observed in the $Ni_2CoCrFeTi_{0.15}Al_{15}$ and $Ni_2CoCrFeTi_{0.2}Al_{0.1}$ HEAs for particle size and number density evolutions, as shown in Fig. 2b and c. However, some $L1_2$ particles in the $Ni_2CoCrFeTi_{0.2}Al_{0.1}$ HEA evolved slowly from spheres to cubes with round corners when the aging time increases, as pointed by the arrows in Fig. 2(c4). This transition is due to the larger contributions of elastic energy caused by the increase of lattice misfit (Table 1) [25].

The quantified information from these images are presented in Fig. 3. As shown in Fig. 3(a), the volume fraction of the $L1_2$ phases kept constant with the increase of aging time in all the three HEAs, indicating that the nucleation process had finished and the $L1_2$ phase started to coarsen after 24 h. The volume fraction of the $L1_2$ phase in the three HEAs are 0.129, 0.151, and 0.186, respectively.

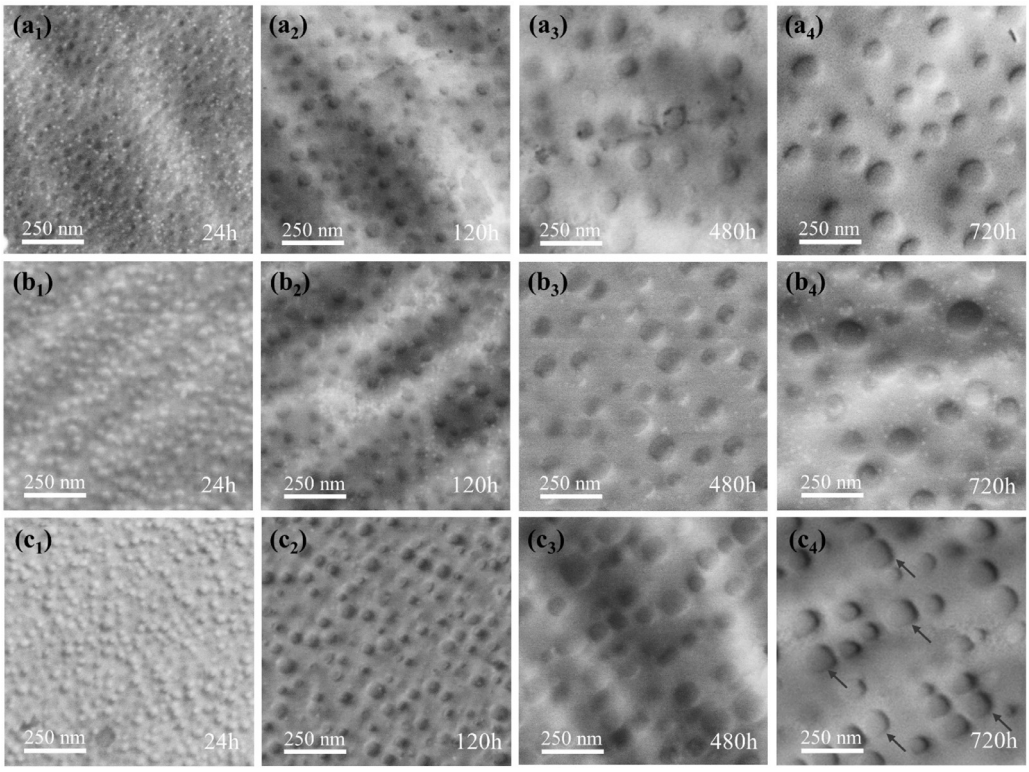

Fig. 2. SEM-BSE images of the $Ni_2CoCrFeTi_xAl_y$ HEAs aged at 800 °C for different time; (a) $Ni_2CoCrFeTi_{0.1}Al_{0.2}$ HEA, (b) $Ni_2CoCrFeTi_{0.15}Al_{0.15}$ HEA, (c) $Ni_2CoCrFeTi_{0.2}Al_{0.1}$ HEA. The $L1_2$ phases in HEAs with lower lattice misfit values remain spherical during aging while in HEA with higher lattice misfit values evolve into round-corner cubes.

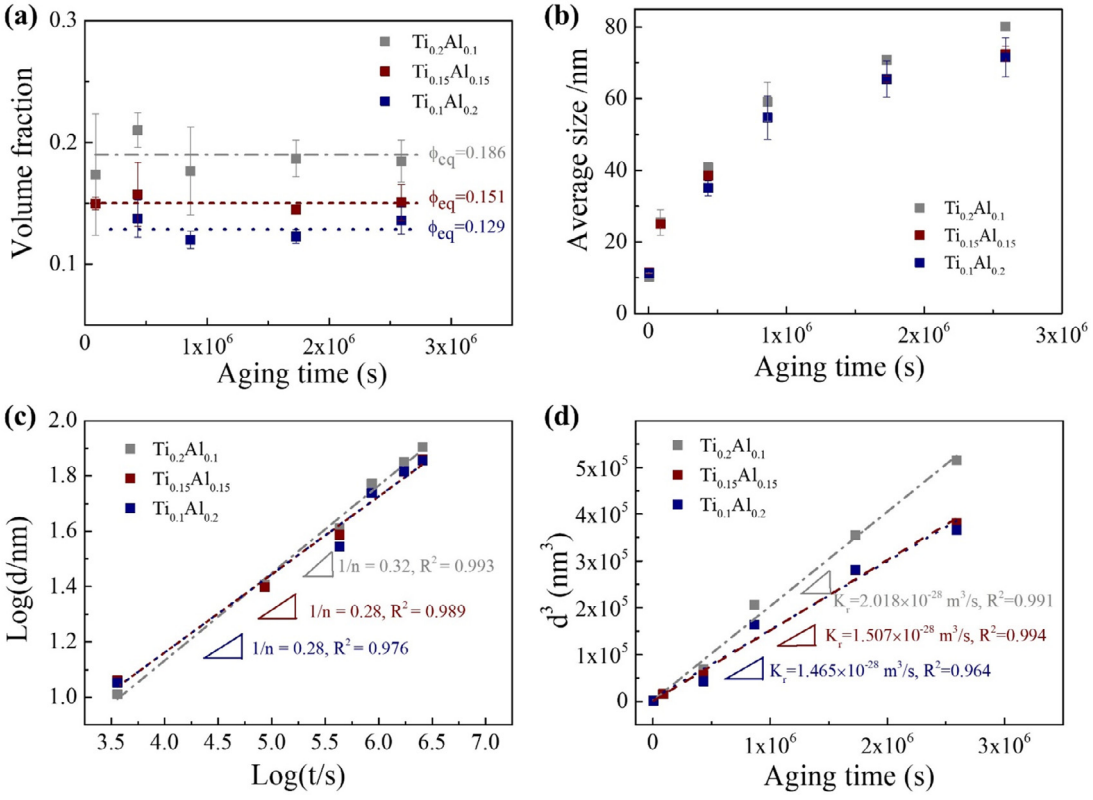

Fig. 3. Precipitation behaviors of the $Ni_2CoCrFeTi_xAl_y$ HEAs aged at 800 °C; (a) the volume fraction evolution of $L1_2$ phase, (b) the average size evolution of $L1_2$ phase. (c) the plots between log(d) vs. log(t) give temporal exponents of average precipitate size evolution which are equivalent to the exponent in modified LSW, (d) The LSW relationship illustrating the coarsening kinetics.

Table 1
Lattice parameters of matrix and $L1_2$ phase, lattice misfits between these two phases (ε), volume fraction (φ), and coarsening constants of the $L1_2$ phase at 800 °C.

HEAs	a_{L12}	a_m	φ	$\lvert\varepsilon\rvert$	K_φ (m^3/s)	K_{LSW} (m^3/s)	Notes
$(NiCoCrFe)_{94}Ti_2Al_4$	–	–	0.127	0.26%	1.82×10^{-28}	0.923×10^{-28}	Ref. [9]
$Ni_2CoCrFeTi_{0.2}Al_{0.1}$	0.35745 nm	0.35830 nm	0.186	0.24%	2.02×10^{-28}	0.925×10^{-28}	Present
$Ni_2CoCrFeTi_{0.15}Al_{0.15}$	0.35764 nm	0.35843 nm	0.151	0.22%	1.51×10^{-28}	0.732×10^{-28}	Present
$Ni_2CoCrFeTi_{0.1}Al_{0.2}$	0.35734 nm	0.35802 nm	0.129	0.19%	1.47×10^{-28}	0.742×10^{-28}	Present
$(CoCrNi)_{94}Ti_3Al_3$	–	–	0.16	0.096%	0.98×10^{-28}	0.468×10^{-28}	Ref. [10]
Ni-17.6Cr-9.7Al	–	–	0.35	–	34.1×10^{-28}	12.9×10^{-28}	Ref. [9]
Ni-21.7Co-13.4Al	–	–	0.23	–	21.2×10^{-28}	9.1×10^{-28}	Ref. [9]
Nimonic PE16	–	–	0.082	–	7.51×10^{-28}	4.2×10^{-28}	Ref. [9]

This variation of volume fraction of the $L1_2$ phase can be explained by the fact that solubility of Ti is larger than that of Al in the NiCoCrFe matrix [26]. Fig. 3(b) shows the average size evolution with aging time of the three HEAs and indicates that the $L1_2$ particle in the HEA with a higher lattice misfit coarsens quicker than those with lower lattice misfit. To obtain the quantified coarsening constant, the modified LSW theory was applied [27]:

$$d^3(t) - d^3(t_0) = K_\varphi (t - t_0) \tag{1}$$

where $d(t)$ represents the average particle size at aging time t, $d(t_0)$ is the average particle size at the time t_0 when coarsening starts, K_φ is the coarsening constant, and t is the aging time. The log(d) vs. log(t) plots for the three HEAs are presented in Fig. 3(c) and their slopes give the exponent values (1/n) of 0.32, 0.28, and 0.28, suggesting that the variation of lattice misfit does not change the cubic law of coarsening. The coarsening is controlled by volume diffusion with $n = 3$, consistent with previous findings [9–12]. The variations of d^3 as a function of t are plotted in Fig. 3(d) and the coarsening constants at 800 °C for the three HEAs are determined to be 2.018×10^{-28}, 1.508×10^{-28}, and 1.465×10^{-28} m^3/s using the linear regression analysis. These values are located within the previously reported range [9–11], as shown in Table 1. One can see that the coarsening constant in these HEAs decreases as the lattice misfit decreases. Although there are many factors affect the value of K_φ, it is reasonable for the present well-designed HEAs to ignore the difference in effective diffusivities and interfacial energies among these HEAs for the following reasons: their component elements are the same; the $L1_2$ phases in these HEAs are all M_3(Ti,Al) type [9,10]; the total contents of Ti and Al are all ~6 at.%, and it has been reported that the Ti/Al ratio has minor effect on the coarsening of $L1_2$ phase [9,10,28]. Accordingly, the difference in K_φ values among these HEAs is attributed to the differences in volume fraction and lattice misfits.

Table 1 shows the coarsening constants of $L1_2$ phases in different alloys. It is clear that the volume fraction of $L1_2$ phases in the $(NiCoCrFe)_{94}Ti_2Al_4$ and $Ni_2CoCrFeTi_{0.1}Al_{0.2}$ HEAs are almost the same, but the coarsening constants are quite different. When the volume fraction of $L1_2$ phase increased from 0.129 to 0.16, taking $Ni_2CoCrFeTi_{0.1}Al_{0.2}$ and $(CoCrNi)_{94}Ti_3Al_3$ HEAs as example, the coarsening constant decreased by one third, while previous studies indicated that a higher volume fraction would lead to a larger coarsening constant [29–31]. Therefore, we believe the lattice misfit plays a more important role in the coarsening of $L1_2$ phase in HEAs. In order to analyze the effect of lattice misfit alone, we then corrected the effect of volume fraction on the coarsening constant. Several researchers have modified the coarsening model as a function of volume fraction $f(\varphi)$ [29–31], among which the model of Wang et al. [32,33] has been well verified by experiments in recent years. The reasonable agreement of the stable PSD curves between the experimental data and theoretical prediction in Fig. 4(a) indicated that Wang's model is feasible for the $L1_2$ phase in HEAs. Thus the corrected coarsening constants (K_{LSW}) of the $L1_2$ phase in different alloy systems are obtained based on Wang's model [33],

$$\frac{K_\varphi}{K_{LSW}} = \frac{27}{4}\left[\frac{2-\left(1-\sqrt{3\varphi}\right)\left(1-\frac{1}{\sqrt{3\varphi}}+\sqrt{\frac{1}{3\varphi}+\frac{1}{\sqrt{3\varphi}}+1}\right)}{\left(1-\frac{1}{\sqrt{3\varphi}}+\sqrt{\frac{1}{3\varphi}+\frac{1}{\sqrt{3\varphi}}+1}\right)^3}\right] \tag{2}$$

The values of K_{LSW} for multicomponent $L1_2$ phase in HEAs are listed in Table 1. It is further confirmed that the coarsening kinetics of $L1_2$ phase in HEAs is much slower compared to that in traditional alloys. As suggested by previous studies [9,11,34], the sluggish diffusion of component elements is the main reason for this slow coarsening kinetics, but the results here revealed the important role of lattice misfit on the coarsening kinetics. As shown in Table 1, the corrected coarsening constant (K_{LSW}) of multicomponent $L1_2$ phase increased from ~0.47×10^{-28} to 0.74×10^{-28} and 0.92×10^{-28} m^3/s when the lattice misfit increased from ~0.1% to ~0.2% and ~0.25%. This trend is not expected for traditional $L1_2$ phase. Recent simulation studies showed that the increase of lattice misfit would decrease the coarsening constant in the Ni–Al system because the elastic energy would decrease the driving force for coarsening [18,35]. In traditional superalloys it has been reported that the influence of lattice misfit on coarsening kinetics can be ignored when its absolute value is small enough (<0.4%) [28]. Although evidences for the proportional relation between coarsening kinetics and lattice misfit have been reported, this just occurs when the lattice misfits are quite large (≥0.4%) [19,20]. Larala et al. [15] theoretically considered that the increase of lattice misfit can either increase or decrease the coarsening kinetics due to its indefinite influence on interfacial energy and equilibrium compositions of phases. Two possible reasons for the anomalous effect in HEAs are suggested: firstly, the increased lattice misfit leads to higher diffusion coefficients; secondly, the interfacial energy between multicomponent $L1_2$ phase and matrix may be related to the magnitude of lattice misfit. In the future, simulation studies are needed to further check these two possibilities since experimental methods are highly limited in measuring the effective diffusivity and interfacial energy.

The lattice misfit also affects the shape of particle size distribution (PSD) curves of the multicomponent $L1_2$ phase. Fig. 4 presents the PSD evolution of the $L1_2$ particle in the three HEAs with aging time. Theoretically predicted PSD curves are also shown as a comparison. The shapes of the PSD curves change with aging time but finally become stable at the aging time of 720 h for all the three HEAs. It is clear that the LSW theory cannot predict the PSD curves of HEAs very well while the prediction of Wang's model agrees with the experimental data to some degree when the lattice misfit is small (Fig. 4a). As the lattice misfit increases, the maximum value of the PSD curves become smaller than that of Wang's prediction, as demonstrated in Fig. 4b and c. Since the effect of volume fraction has already been considered, the decrease of the maximum value of the PSD curves should be caused by the

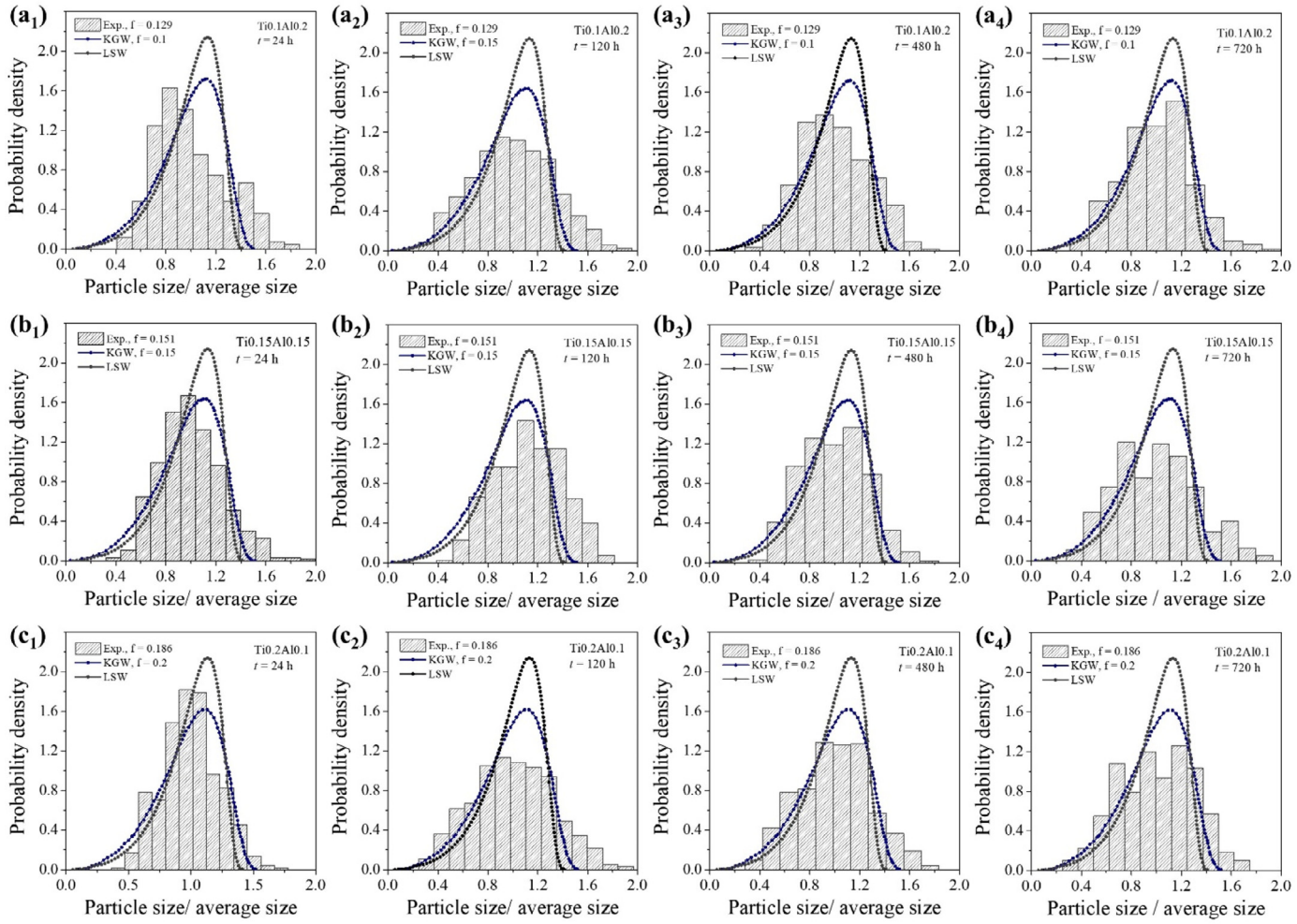

Fig. 4. The particle size distributions (PSDs) of $Ni_2CoCrFeTi_xAl_y$ HEAs aged at 800 °C for 24–720 h; (a) $Ni_2CoCrFeTi_{0.1}Al_{0.2}$ HEA, (b) $Ni_2CoCrFeTi_{0.15}Al_{0.15}$ HEA, (c) $Ni_2CoCrFeTi_{0.2}Al_{0.1}$ HEA.

increase of lattice misfit. This trend is similar with most reported experimental and simulation studies [17,19,35].

In summary, the effect of lattice misfit on the coarsening behavior of multicomponent $L1_2$ phase in HEAs are experimentally investigated. A decreasing lattice misfit results in a significant decrease of coarsening kinetics of $L1_2$ phase in HEAs. This relation between lattice misfit and coarsening kinetics is quite different from that of precipitates in traditional alloys. Because of this remarkable influence of lattice misfit on the coarsening kinetics, the small lattice misfit between $L1_2$ phase and matrix in HEAs should also be a key reason for the superior coarsening resistance of $L1_2$ phase in HEAs. A decrease of maximum value of PSD curves with increasing lattice misfit is also observed. These findings provide a new sight of understanding the excellent thermal stability of multicomponent $L1_2$ phase in HEAs.

Declaration of Competing Interest

The authors declare that they have no known competing financial interests or personal relationships that could have appeared to influence the work reported in this paper.

Acknowledgements

The authors are grateful for the financial support from the Hong Kong Research Grant Council (JJK, Hong Kong Grant No. CityU 11212915 and CityU 11205018] and National Natural Science foundation of China (ZJW, Grant No. 51771149).

Supplementary materials

Supplementary material associated with this article can be found, in the online version, at doi:10.1016/j.scriptamat.2020.03.030.

References

[1] J.W. Yeh, S.K. Chen, S.J. Lin, J.Y. Gan, T.S. Chin, T.T. Shun, C.H. Tsau, S.Y. Chang, Adv. Eng. Mater. 6 (5) (2004) 299–303.
[2] E.P. George, W.A. Curtin, C.C. Tasan, Acta Mater. (2019).
[3] T. Yang, Y.L. Zhao, Y. Tong, Z.B. Jiao, J. Wei, J.X. Cai, X.D. Han, D. Chen, A. Hu, J.J. Kai, K. Lu, Y. Liu, C.T. Liu, Science 362 (6417) (2018) 933–937.
[4] J. Li, C. Guo, Y. Ma, Z. Wang, J. Wang, Acta Mater. 90 (2015) 10–26.
[5] A. Baldan, J. Mater. Sci. 37 (11) (2002) 2171–2202.
[6] A. Baldan, J. Mater. Sci. 37 (12) (2002) 2379–2405.
[7] F. He, Z. Wang, Q. Wu, J. Li, J. Wang, C.T. Liu, Scr. Mater. 126 (2017) 15–19.
[8] F. He, D. Chen, B. Han, Q. Wu, Z. Wang, S. Wei, D. Wei, J. Wang, C.T. Liu, J.-j. Kai, Acta Mater. 167 (2019) 275–286.
[9] Y.Y. Zhao, H.W. Chen, Z.P. Lu, T.G. Nieh, Acta Mater. 147 (2018) 184–194.
[10] Y. Zhao, T. Yang, B. Han, J. Luan, D. Chen, W. Kai, C.T. Liu, J.-j. Kai, Mater. Res. Lett. 7 (4) (2019) 152–158.
[11] P. Pandey, S. Kashyap, D. Palanisamy, A. Sharma, K. Chattopadhyay, Acta Mater. (2019).
[12] H. Peng, L. Hu, L. Li, W. Zhang, Mater. Sci. Eng. 772 (2020) 138803.
[13] W. Lu, C.H. Liebscher, F. Yan, X. Fang, L. Li, J. Li, W. Guo, G. Dehm, D. Raabe, Z. Li, Acta Mater. 185 (2020) 218–232.
[14] P.H. Leo, R.F. Sekerka, Acta Metall. 37 (12) (1989) 3139–3149.

[15] V. Larala, W.C. Johnson, P.W. Voorhees, Scr. Metall. 23 (10) (1989) 1749–1754.
[16] M. Fährmann, P. Fratzl, O. Paris, E. Fährmann, W.C. Johnson, Acta Metall. Mater. 43 (3) (1995) 1007–1022.
[17] V. Vaithyanathan, L.Q. Chen, Acta Mater. 50 (16) (2002) 4061–4073.
[18] C. Liu, Y. Li, L. Zhu, S. Shi, J. Mater. Eng. Perform. 27 (9) (2018) 4968–4977.
[19] S. Iwamura, Y. Miura, Acta Mater. 52 (3) (2004) 591–600.
[20] J.G. Conley, M.E. Fine, J.R. Weertman, Acta Metall. 37 (4) (1989) 1251–1263.
[21] P. Pandey, S.K. Makineni, A. Samanta, A. Sharma, S.M. Das, B. Nithin, C. Srivastava, A.K. Singh, D. Raabe, B. Gault, K. Chattopadhyay, Acta Mater. 163 (2019) 140–153.
[22] D. Mukherji, R. Gilles, B. Barbier, D.D. Genovese, B. Hasse, P. Strunz, T. Wroblewski, H. Fuess, J. Rösler, Scr. Mater. 48 (4) (2003) 333–339.
[23] Z.J. Wang, Q.F. Wu, W.Q. Zhou, F. He, C.Y. Yu, D.Y. Lin, J.C. Wang, C.T. Liu, Scr. Mater. 162 (2019) 468–471.
[24] M.V. Nathal, R.A. Mackay, R.G. Garlick, Mater. Sci. Eng. 75 (1) (1985) 195–205.
[25] T. Wang, G. Sheng, Z.-K. Liu, L.-Q. Chen, Acta Mater. 56 (19) (2008) 5544–5551.
[26] F. He, Z. Wang, B. Han, Q. Wu, D. Chen, J. Li, J. Wang, C.T. Liu, J.J. Kai, J. Alloy. Compd. 769 (2018) 490–502.
[27] C.J. Kuehmann, P.W. Voorhees, Metall. Mater. Trans. A 27 (4) (1996) 937–943.
[28] X. Li, N. Saunders, A.P. Miodownik, Metall. Mater. Trans. A 33 (11) (2002) 3367–3373.
[29] J. Marqusee, J. Ross, J. Chem. Phys. 80 (1) (1984) 536–543.
[30] A. Ardell, Phys. Rev. B 41 (4) (1990) 2554.
[31] C.K.L. Davies, P. Nash, R.N. Stevens, Acta Metall. 28 (2) (1980) 179–189.
[32] K.G. Wang, M.E. Glicksman, K. Rajan, Phys. Rev. E 69 (6) (2004) 061507.
[33] B.A. Pletcher, K.-G. Wang, M.E. Glicksman, Int. J. Mater. Res. 103 (11) (2012) 1289–1293.
[34] K.Y. Tsai, M.H. Tsai, J.W. Yeh, Acta Mater. 61 (13) (2013) 4887–4897.
[35] H.J. Ryu, S.H. Hong, J. Weber, J.H. Tundermann, J. Mater. Sci. 34 (2) (1999) 329–336.